NASA/Aura/Microwave Limb Sounder Water Vapor Validation at Mauna Loa Observatory by Raman Lidar

John E. Barnes[1], Trevor Kaplan[1], Holger Vömel[2] and William G. Read[3]

[1]NOAA/ESRL/ Global Monitoring Division/Mauna Loa Observatory, 1437 Kilauea Ave., Hilo, HI 96720, 808-933-6965, E-mail: John.E.Barnes@noaa.gov

[2]University of Colorado and NOAA/ESRL/GMD, Boulder, CO

[3] Jet Propulsion Laboratory, California Institute of Technology, Pasadena, CA

To be submitted to JGR, April 2007, for special Aura validation issue.

Corresponding Author:

John E. Barnes

NOAA/Mauna Loa Observatory

1437 Kilauea Ave.

Hilo, HI 96720

808-933-6965 ext 222

808-933-6967 FAX

John.E.Barnes@noaa.gov

Abstract

The NASA/Aura/Microwave Limb Sounder (MLS) instrument has been compared to the Mauna Loa Observatory Raman water vapor lidar. Calibration of the lidar used Vaisala RS80-H radiosondes launched from the observatory. The average standard deviation between the sondes and the lidar, in the range 6 km to 11.5 km, is 11.9%. The sondes indicate no overlap correction for the lidar at low altitudes is necessary. A comparison was made between the lidar total column water and a GPS total column water measurement as a check on the calibration, resulting in a correlation slope of 1.026+/- 0.058 and $R^2 = 0.84$. The MLS measurements are significantly better in the stratosphere where the lidar has poor sensitivity. The MLS measurement in the troposphere has much lower altitude resolution than the lidar so the validation overlap altitudes are limited. A comparison is made with version 1.5 MLS data for 32 overpasses at the three MLS altitudes in the troposphere. The GPS total column water measurement was used to screen the overpasses by eliminating ones where the water varied by more than 50% during the lidar integration period. At 147 hPa the MLS data show a dry bias of 44.8% +/- 36%. At 215 hPa the MLS measurement also shows a dry bias of 22.3% +/- 22% and at 316 hPa there is a dry bias of 19.9% +/- 46%. The dry bias seen is consistent with the Cryogenic Frost-Point Hygrometer (CFH) measurements at many latitudes (23% +/- 37% at 215 hPa and 4% +/- 62% at 316 hPa).

1. Introduction

Tropospheric water vapor measurements from the Microwave Limb Sounder (MLS) on the NASA/Aura satellite have been compared with a Raman water vapor lidar at the National Oceanic and Atmospheric Administration's Mauna Loa Observatory (MLO). Mauna Loa Observatory is a high-altitude climate-monitoring observatory located at 19.54^{o}N and 155.58^{o}W

at an altitude of 3397 m above sea level. It is a primary location for the Network for the Detection of Atmospheric Composition Change. The air above MLO ranges from true tropical air masses to mid-latitude air depending on circulation patterns and can switch between the two in a few days (*Barnes and Hofmann*, 2001). The observatory is often on the boundary of these two air masses (*Grant, et. al.* 1996). The tropopause, as measured by radiosonde, reaches the highest altitudes (approximately 17.5 km) in northern hemisphere winter and lowest (approximately 16 km) in the summer as it does in tropical regions. The stratospheric zonal winds however, follow an annual cycle as in the mid-latitudes, and the quasibiennial oscillation is a second-order effect in the winds. MLO also lies at a longitude which experiences the most mid-latitude intrusions into the tropical upper troposphere (*Waugh and Polvani*, 2000). In addition to water vapor; aerosols, ozone, temperature and winds are measured by lidars at MLO. Other remotely sensed trace gases include nitric acid, NO_2, BrO. Because of the high altitude many free tropospheric measurements can be made in-situ at the observatory including aerosols, solar radiation, greenhouse gases, ozone-depleting molecules and radon.

The MLS was launched on 15 July, 2004 and has been making measurements since 13 August, 2005. The microwave limb scanning technique observes millimeter- and submillimeter-wavelength-thermal emissions as the instrument field of view is scanned through the limb of the atmosphere (*Waters et. al.*, 2006). The MLS instrument has a horizontal resolution of about 200 km and can observe day and night, and in the presence of clouds. The MLO lidar is limited to nighttime observations, can only penetrate thin cirrus and has much higher vertical resolution than the MLS instrument. The horizontal resolution for the lidar is harder to specify, but is related to the transport of the air above the lidar during the integration period. The winds will vary with altitude in both speed and direction. The data files are saved every few minutes and

added to improve the measurement error. An advantage of lidar measurements is that short term variations can be examined to determine how much a given parameter was changing during the entire integration period.

2. Lidar

Lidar aerosol measurements have been made at MLO since the mid 1970's, first with a Ruby-laser-based system (*DeFoor and Robinson*, 1987), and starting in 1994 a Nd:YAG-laser-based system (*Barnes and Hofmann*, 1997). The data are submitted to the Network for the Detection of Atmospheric Composition Change database. Aerosol backscatter is measured at both 532 and 1064 nm. The 1064 nm channel is especially sensitive to sub-visible cirrus. Raman channels for nitrogen (607 nm) and water vapor (660 nm) were added in 2002. The Raman scattered light is from the incident 532 nm laser light scattering off of the nitrogen and water molecules. These two channels use a separate 74 cm diameter parabolic mirror with the optics and photomultiplier tubes located just above the prime focus of the mirror. The detectors used for both channels are H7421-40 Hamamatsu photon-counting heads. The detector assembly is small and blocks about the same amount of light that a Newtonian-type secondary mirror would if present.

A single lens collimates the light which then passes through a Semrock notch filter which reduces the 532 nm light by >6 optical depths (10^6). The two Raman wavelengths are then split using a long-wavelength-pass edge filter reducing the 532 nm light in the water vapor channel by an additional >2 optical depths. The two light paths then pass through interference filters which reject the 532 nm light by >6 optical depths. The large rejection (>14 optical depths) of the 532

92 nm (Rayleigh and aerosol) scattered light from the water vapor detector is important when trying
93 to measure a few parts per million with the much weaker Raman scattered light. The two optical
94 paths are designed to be symmetrical, so that both channels will have about the same near-range
95 overlap correction which reduces the signals. These corrections would then cancel in the
96 analysis.

97 The nitrogen channel has an additional neutral density filter (2 optical depths). This reduces
98 the Raman nitrogen signal to a level where no saturation effects are seen on the detector and the
99 lowest altitude bins can be used. Even with this reduction in nitrogen signal, the measurement
100 error is dominated by the water vapor signal at all altitudes. Although the reduction does limit
101 the channel's usefulness for other lidar applications (e.g. temperature) it optimizes the water
102 vapor measurement. The water vapor system parameters are summarized on Table 1.

103 In the Raman lidar technique (*Melfi*, 1972; *Cooney*, 1970) the water vapor and nitrogen
104 signals are corrected for extinction, which at this high altitude site is generally small, and the
105 ratio of the corrected signals is then proportional to the water vapor mixing ratio. An additional
106 correction (*Halldorsson and Langerhoic*, 1978; *Harms*, 1979) may be needed to account for the
107 overlap between the telescope and laser for the range close to the instrument. The ratio is
108 multiplied by a calibration constant needed to account for uncertainties in transmissions,
109 reflectivities and sensitivities of the optical and electronic components. In this case Vaisala
110 RS80-H radiosonde profiles have been used to derive a single constant. The accuracy of the
111 humidity measurement on radiosondes has been shown to vary with the sensor type and
112 individual instruments. Especially noteworthy is a dry bias (*Farrare et. al*., 1995) at low
113 humidities and a time-lag at low temperatures (*Miloshevic et. al*., 2001; *Milsoshevic et. al*.,
114 2004).

Coincident flights with RS80-H and cryogenic frost-point hygrometers at MLO (Vömel et. al., 2003) have shown that the RS80-H deviates above 11-12 km where the temperature drops below -55 deg C. In order to minimize this effect as well as the dry bias, the radiosondes were flown on relatively wet nights and the upper tropospheric data were not used for the calibration of the lidar. The most recent calibration flight is shown in Figure 1. The radiosonde's relative humidity and temperature have been used to calculate it's mixing ratio, parts per million by volume (ppmv), using the Vaisala recommended conversion (*Hyland and Wexler*, 1983). Note that above 11.5 km the radiosonde doesn't track the layers seen by the lidar. The calibration for mixing ratio, which is the most directly-measured quantity by the lidar, is shown in Figure 2. This is the summary of all calibration flights flown since 2005/10 when the lidar was last modified. The range from 6 to 11.5 km was used to determine the calibration constant. In this altitude range the mixing ratios which are compared vary by about a factor of 40. There is no significant bias with altitude considering the error bars. Between 3.4 (MLO altitude) and 6 km the lidar has incomplete overlap and the data are not used for calibration. The average standard deviation in the calibration range is 11.9%. Below 6 km, the deviation increases, probably due to larger variability in water vapor near the ground. Given the data, error and variability, no low-altitude overlap correction was deemed necessary and none has been applied in this analysis.

As a check on the calibration of the lidar, the water profile has been integrated to compare with a Global Positioning System (GPS) integrated precipitable water (IPW) measurement. The GPS instrument is part of a NOAA/Global Systems Division network (*Gutman et. al.*, 2004) and has been operating at MLO since 2004. The GPS technique measures the total water column along several paths to the GPS satellites. Thirty minutes averages were used to compare with the lidar integration period. A correlation with the GPS for all lidar data taken since 2005/10, which

includes 63 points, is shown in Figure 3. The lidar profile has been integrated from the ground to the highest reliable altitude, usually between 13 and 17 km. Any water vapor above the highest altitude measured by the lidar will not significantly add to the IPW. The correlation shows a very small intercept (-0.18 +/- 0.25 mm) and the slope differs from 1.0 by 0.026+/- 0.058. Note the low levels of IPW that are typical of high altitude sites.

3. MLS Data

At the time that this article was prepared there were 32 overpasses within 4 hours, and 12 within 2 hours of version 1.5 MLS data that could be compared to the lidar. There were only 4 overpasses available for version 2.2 and no significant results could be obtained. Following the recommendations for these data sets, profiles have been screened using the appropriate status flags, precision values, and quality flags. Only profiles with even values of the status field were used, which indicated that the retrieved profile passed a number of rejection criteria. Data were required to have associated quality values larger than 0.9, indicating that for these data a good fit between the observed radiances and those values computed by the forward model using the retrieved values was achieved. Lastly data with negative precision values were rejected, since these data points did not have a sufficient information yield from MLS.

A lidar measurement at a given altitude represents an average over time and over the altitude range in the given bin. The MLO lidar altitude resolution was 300 meters. In order to compare these data with the MLS values the lidar resolution has been degraded to match that of MLS. The basics of this resolution degrading is discussed by *Read et al.* (2007, this issue) where the observed *in situ* profile is multiplied by the forward model smoothing function and the

instrument averaging kernel. In version 1.5 the averaging kernel is nearly a unity matrix, which means that the radiances at levels above and below any reported level do not contribute significantly to the radiances at that level. Therefore, the smoothing is effectively done by the forward model smoothing function only.

At the comparison altitudes the average of the relative differences between the MLS and lidar for 2 hour data did not significantly differ from the 4 hour dataset. This was also found to be true for cryogenic frost-point hygrometer measurements by *Vömel et. al*. (this issue). But the variability (standard deviation) of the relative differences was affected by how the overpasses were further screened. It was found that the variability in the relative differences could be reduced the most by selecting only the 2 hour data, and by also eliminating overpasses where the water vapor was relatively unstable. For this study the GPS IPW was used as a measure of stability. The IPW was examined during the lidar integration period and cases where the IPW varied by more than 55% where not used. Since the IPW is a column measurement this does not guarantee the conditions at each comparison altitude were stable, but it does provide an objective criterion for screening the data. The stability of the MLS data was also examined by calculating the standard deviation for the overpass scan and the scans immediately North and South of the overpass location. The same 55% cut-off was used which eliminated a single overpass.

The relative differences, (MLS-Lidar)/Lidar, for the remaining overpasses for three of the MLS altitudes are shown in Figure 4. The standard deviation is a measure of the variation in the relative differences calculated. The 147 hPa pressure level corresponds to approximately 14.3 km and the MLS data show a dry bias of 44.8% +/- 36%. At 215 hPa (11.9 km) the MLS measurements show a dry bias of 22.3% +/- 22% and are consistent with the dry bias of 23% +/- 37% measured by the Cryogenic Frost-Point Hygrometer (CFH) at many latitudes (*Vömel et. al.,*

this issue). At 316 hPa there is also a dry bias of 19.9% +/- 46% which is consistent with the CFH's 4% +/- 62% measured at many latitudes, but the large spread in the result limits the usefulness for validating MLS.

4. Discussion and Summary

At each of the three altitudes (147, 215, 316 hPa) the variation (36%, 22%, 46%) in the relative difference is larger than the combined error in the lidar and MLS (20%, 11%, 21% respectively). For the 32 overpasses, the lidar errors due to the signal statistics are (16%, 7%, 2%) and the MLS average errors are (11%, 9%, 21%) for the respective altitudes. This would imply that natural variability is a strong factor in the variation. At the 147 hPa altitude the MLS average mixing ratio was 7.3 ppmv and at this altitude and low level of water vapor, the lidar signal-to-noise ratio is low. The large dry bias measured (44.8%) is larger than the CFH result of about 14% (*Vömel et. al.*, this issue) that was measured at many latitudes. Although there is no reason to suspect the lidar data at this pressure, a small background on the water vapor channel would introduce higher water vapor levels in the lidar data, which could explain some of the difference.

For comparison to an MLS observation, the lidar was usually operated for 2 hours. Analysis of radiosonde data show the winds at the altitudes used for validation are generally westerly (9.1 to 16.7 m/s) with a small North-South component (-1.6 to 2.2 m/s). This would mean that during the two hour observation roughly 66 to 120 km of air would be transported over the station. This is less but of the same order as the horizontal resolution of the MLS measurement which is about 200 km. The MLS travels along an orbital track which is close to North-South but looks back

towards the sun. The spacecraft travels about 190 km during a scan (about 25 sec) so there is a difference in the air sampled by the two instruments. This could account for the relatively large variability in the relative difference between the MLS and the lidar especially in the presence of large horizontal gradients in water vapor.

Calibration of the lidar for water vapor has been accomplished using Vaisala RS80-H radiosondes to an accuracy of about +/-12%. The calibration has been verified by comparing the integrated precipitable water with GPS measured values with a correlation of +/-6%. The useful range of the lidar is from 3.4 km (MLO altitude) to nearly 15 km where the mixing ratio is generally below 10 ppmv. The lidar has been shown to be accurate enough for MLS validation in the sense that its measurement error is well below the large variability seen in tropospheric water vapor at this observing site which limits the comparison. Screening the data for stable conditions during the observations significantly reduced the variability in the difference between the MLS and lidar. With a larger dataset further screening might be useful, possibly with back trajectories. It is hoped that enough version 2.2 data will be available to analyze in the future. The higher altitude resolution of the MLS data would allow more comparisons in the effective range of the lidar.

Acknowledgements

We would like to thank Seth Gutman with the NOAA/GSD GPS group for help with data comparisons.

References

Barnes, J. E., and D. J. Hofmann (1997), Lidar measurements of stratospheric aerosol over Mauna Loa Observatory, *Geophys. Res. Lett*., 24, 1923-1926.

Barnes, J. E., and D. J. Hofmann (2001), Variability in the stratospheric background aerosol over Mauna Loa Observatory, *Geophys. Res. Lett*., 28, 2895-2898.

Cooney, J., (1970) Remote measurements of atmospheric water vapor using the Raman component of laser backscatter, *J. Appl. Meteor*., 9, 182-184.

DeFoor, T., and E. Robinson, (1987) Stratospheric lidar profiles from Mauna Loa Observatory during winter 1985-1986, *Geophys. Res. Lett*., 14, 618-621.

Farrare, R. A., S. H. Melfi, D. N. Whiteman, K. D. Evans, F. J. Schmidlin, and D. O'C. Starr, (1995) A comparison of water vapor measurements made by Raman lidar and radiosondes, *J. Atmos. Oceanic Technol*., 12, 1177-1195.

Grant, W. B., E. Y. Browell, C. S. Long, L. L. Stowe, R. G. Grainger, and A. Lambert (1996), Use of volcanic aerosols to study the tropical stratospheric reservoir, *J. Geophys. Res*., 101, 3973-3988.

Gutman, S. I., S.R. Sahm, S.G. Benjamin, B.E. Schwartz, K.L. Holub, J.Q. Stewart, and T.L. Smith (2004), Rapid Retrieval and Assimilation of Ground Based GPS Precipitable Water Observations at the NOAA Forecast Systems Laboratory: Impact on Weather Forecasts. *Journal of the Meteorological Society of Japan*, Vol. 82, No. 1B, pp. 351-360.

Halldorsson, T., and J. Langerhoic, (1978) Geometrical form factors for the lidar function, *Applied Optics*, 17, 240-244.

Harms, J., (1979) Lidar return signals for coaxial and noncoaxial systems with central obstruction, *Applied Optics*, 18, 1559-1566.

Hyland, R. W. and A. Wexler (1983), Formulations for the Thermodynamic Properties of the saturated Phases of H2O from 173.15K to 473.15K, *Ashrae Trans*, 89(2A), 500-519.

Melfi, S. H., (1972) Remote measurements of the atmosphere using Raman scattering, *Applied Optics*, 11, 1605-1610.

Miloshevich, L. M., H. Vömel, A. Paukkunen, A. J. Heymsfield, and S. J. Oltmans, (2001) Characterization and correction of relative humidity measurements from Vaisala RS80-A radiosondes at cold temperatures, *J. Atmos. Oceanic Technol*., 18, 135-156.

Miloshevich, L. M., A. Paukkunen, H. Vömel, and S. J. Oltmans, (2004) Development and validation of a time-lag correction for Vaisala radiosonde humidity measurements, *J. Atmos. Oceanic Technol*., 21, 1305-1327.

Read, W. G. et al. (2007), EOS Aura Microwave Limb Sounder Upper Tropospheric and Lower Stratospheric Humidity Validation, *J. Geophys. Res.*, this issue.

Vömel, H., D., M. Fujihara, M. Shiotani, F. Hasebe, S. Oltmans, J. E. Barnes, (2003) The behavior of the Snow White chilled-mirror hygrometer in extremely dry conditions, *J. Atmos. Oceanic Technol*., 20, 1560-1567.

Vömel, H., D. David, and K. Smith (2007), Accuracy of Tropospheric and stratospheric water vapor measurements by the Cryogenic Frost point Hygrometer (CFH): Instrumental details and observations, *J. Geophys. Res*, 112, D08305.

Vömel, H. et. al. (2007), Validation of Aura/MLS water vapor by balloon borne cryogenic frostpoint hygrometer measurements, *J. Geophys. Res*., this issue.

273 Waugh D. W., and L. M. Polvani (2000), Climatology of intrusions into the tropical upper
274 troposphere, *Geophys. Res. Lett*., 27, 3957-3860.
275 Water, J. W. et al. (2006), The Earth Observing System Microwave Limb Sounder (EOS MLS)
276 on the Aura satellite, *IEEE Transactions on Geoscience and Remote Sensing*, 44, 1075-1092.

Table

Maximum laser energy at 532 nm	0.67 Joule/pulse
Pulse repetition frequency	30 Hz
Laser divergence, full angle	< 1 mrad
Telescope diameter	74 cm
Telescope focal length (F4.5)	333 cm
Nitrogen filter at 607 nm	1 nm FWHH
Water vapor filter at 660 nm	1 nm FWHH
Detection field of view, full angle	1 mrad
Altitude resolution	300 m

Table 1. MLO Raman lidar description.

Figure captions

Figure 1. Radiosonde flight for calibration of the lidar on 2007/3/6. Also shown are the MLS version 2.2 mixing ratios from the overpass.

Figure 2. Vaisala RS80-H radiosonde, lidar difference (Sonde-Lidar)/Sonde. Error bars indicate one standard deviation of the lidar precision. Dotted lines at +/- 11.9% are estimated accuracy of lidar including calibration error.

Figure 3. GPS and Lidar integrated precipitable water (IPW). The slope is 1.026 +/-0.058 and the intercept is -0.18+/- 0.25 mm.

Figure 4. Relative difference between MLS v1.5 and MLO Raman lidar water vapor at 147, 215 and 316 hPa for 32 overpasses. The solid lines show the average and +/- one standard deviation. The dotted line indicates the median.

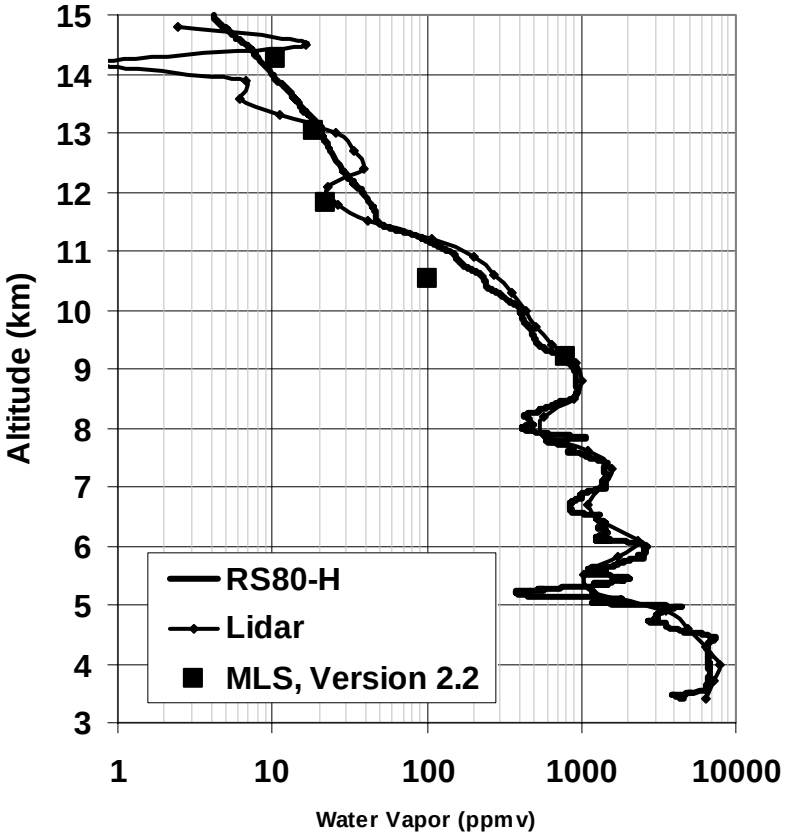

Figure 1. Radiosonde flight for calibration of the lidar on 2007/3/6. Also shown are the MLS version 2.2 mixing ratios from the overpass.

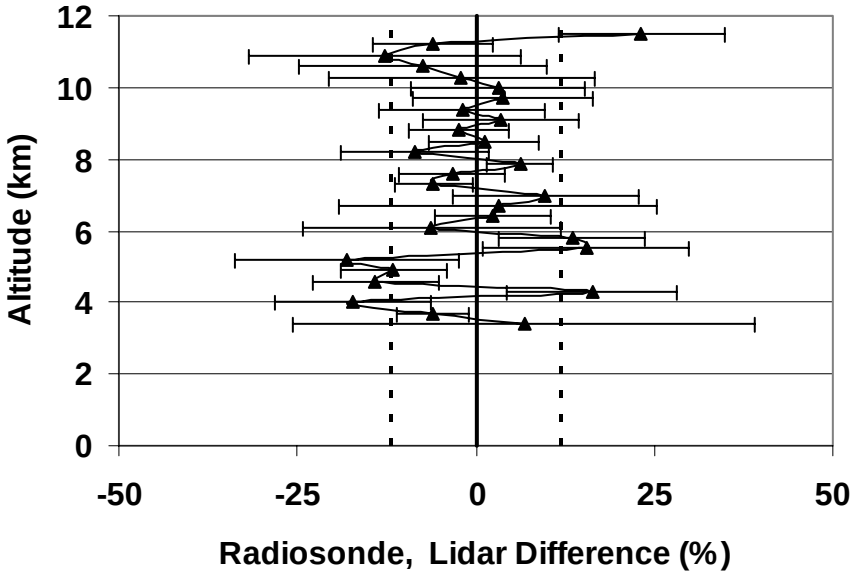

Figure 2. Vaisala RS80-H radiosonde, lidar difference (Sonde-Lidar)/Sonde. Error bars indicate one standard deviation of the lidar precision. Dotted lines at +/- 11.9% are estimated accuracy of lidar including calibration error.

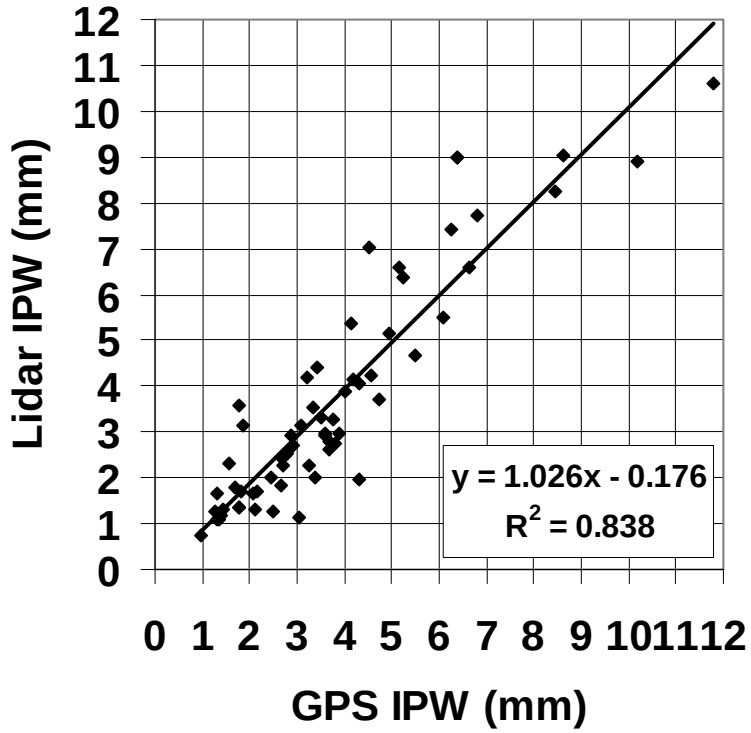

Figure 3. GPS and Lidar integrated precipitable water (IPW). The slope is 1.026 +/-0.058 and the intercept is -0.18+/- 0.25 mm.

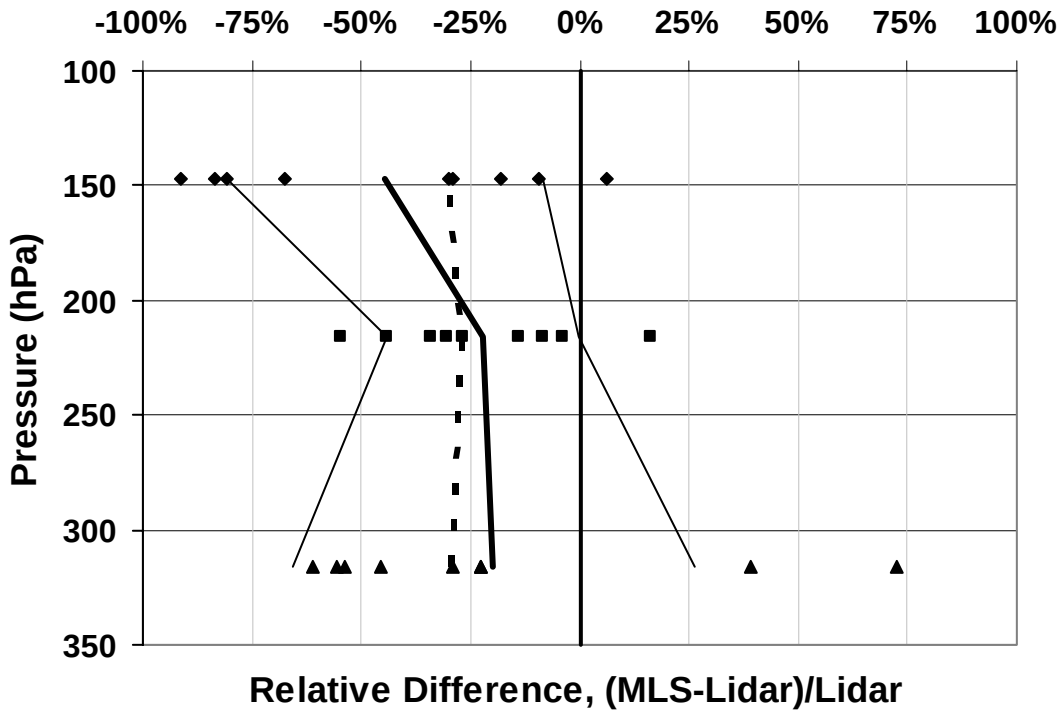

Figure 4. Relative difference between MLS v1.5 and MLO Raman lidar water vapor at 147, 215 and 316 hPa for 32 overpasses. The solid lines show the average and +/- one standard deviation. The dotted line indicates the median.